arXiv:cond-mat/9711025v2 [cond-mat.mes-hall] 7 Sep 1998

Finite voltage shot noise in normal-metal – superconductor junctions

Alban L. Fauchère[a], Gordey B. Lesovik[b], and Gianni Blatter[a]
[a] *Theoretische Physik, Eidgenössische Technische Hochschule, CH-8093 Zürich, Switzerland*
[b] *Institute of Solid State Physics, Chernogolovka 142432, Moscow district, Russia*
(March 13, 1998)

We express the low-frequency shot noise in a disordered normal-metal – superconductor (NS) junction at finite (subgap) voltage in terms of the normal scattering amplitudes and the Andreev reflection amplitude. In the multichannel limit, the conductance exhibits resonances which are accompanied by an enhancement of the (differential) shot noise. In the study of multichannel single and double barrier junctions we discuss the noise properties of coherent transport at low versus high voltage with respect to the Andreev level spacing.

Shot noise arises from the current fluctuations in transport as a consequence of the discrete nature of the carriers, first predicted by Schottky for the vaccuum tube[1]. In a coherent conductor the quantum fluctuations, which follow from the probabilistic nature of the backscattering restricted by the Pauli principle, are reduced in comparison to the Schottky result[2]. In a disordered normal-metal – superconductor (NS) junction, the shot noise is produced by the normal scattering processes as well as the imperfect Andreev reflection[3–6]. The Andreev reflection introduces fluctuations proportional to the double electron charge, which may be iteratively increased to give fluctuations of several charge quanta in biased SNS junctions[7]. In this paper we study the shot noise at finite voltage in a disordered NS junction as well as its structure due to the iterative scattering processes between the disordered normal lead and the NS interface. We derive a general formula which expresses the differential shot noise of the dirty NS junction in terms of the scattering matrix of the normal lead and the (scalar) amplitude of Andreev reflection. In the models of a single barrier normal-metal – insulator – normal-metal – superconductor (NINS) junction and a double barrier NINIS junction, we explain the existence of a non-trivial resonance structure.

We consider a disordered NXS junction, shown in the inset of Fig. 1, with an arbitrary elastic scattering region X in the normal lead, whose effect on the noise is to be determined. The low-frequency power spectrum of the current fluctuations is determined by the irreducible current–current correlator

$$P = \int dt\, e^{i\omega t} \langle\langle I(t)\, I(0) \rangle\rangle, \qquad \omega \to 0 \tag{1}$$

($\langle\langle I(t)\, I(0)\rangle\rangle = \langle (I(t) - \langle I \rangle)\,(I(0) - \langle I \rangle)\rangle$ is the second cumulant in time). The time-dependence of the current operator is defined by

$$I(t) = \exp\left[i\,(H - \mu N)\, t\right]\, I\, \exp\left[-i\,(H - \mu N)\, t\right]. \tag{2}$$

In the mean field approximation for the Hamiltonian H we do not account for the fluctuations of the order parameter in the S region. The effective Hamiltonian is diagonalized by a Bogoliubov transformation[8]. After integration over the cross-section, the net current operator can be expressed through the positive energy eigenfunctions,

$$I(t) = \frac{-e}{mi} \sum_{\epsilon_m, \epsilon_n > 0} \int dydz \big(u_m^* \hat{\partial}_x u_n \gamma_m^\dagger \gamma_n - v_m^* \hat{\partial}_x v_n \gamma_n \gamma_m^\dagger \big) e^{i(\epsilon_m - \epsilon_n)t} \tag{3}$$

which may be evaluated in the normal lead. The operators γ_m belonging to the wavefunctions (u_m, v_m) annihilate the scattering states of the disordered NS junction (note $u\hat{\partial}_x v = u\partial_x v - v\partial_x u$). We note that the symmetry of the BdG eigenfunctions (u_n, v_n), ϵ_n with respect to sign reversal of energy to $(-v_n^*, u_n^*)$, $-\epsilon_n$ is the consequence of spin degeneracy in Nambu space, allowing the the negative energy states to be eliminated in favor of the positive energy states.

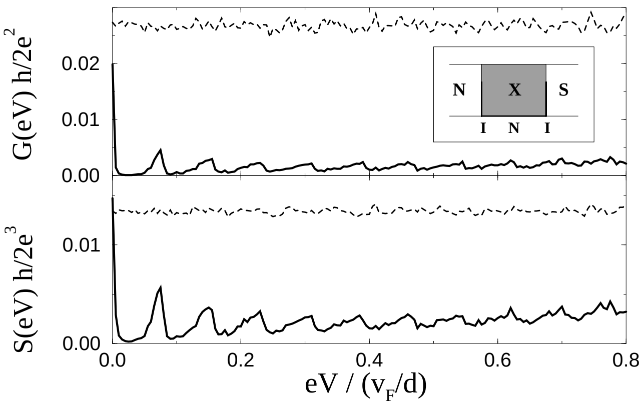

FIG. 1. Differential conductance (top) and shot noise (bottom) in a multichannel NINIS junction (see inset, symmetrical barriers of strength $\int dx\, V(x) = 3\hbar v_F$, $T_1 = T_2 \approx 0.05$, interbarrier distance $d = 20\, v_F/\Delta$, 8×10^4 channels). The average shot noise per channel [Eq. (6)] exhibits maxima at the resonances of the conductance (solid lines). Note the enhanced structure of the noise with respect to the conductance [Eq. (5)]. The dashed lines show the corresponding results for the normal state NININ junction. Inset: schematic NXS junction, e.g., X = INI.

At voltages below the superconducting gap ($eV < \Delta$), the quasi-particles are injected from the normal reservoir only, and the wavefunctions depend on the $N \times N$ reflection matrices $r_{ee}(\epsilon)$, $r_{he}(\epsilon)$, $r_{eh}(\epsilon)$, and $r_{hh}(\epsilon)$ of the entire disordered NS junction[9]. The scattering states indexed by $m = [{}^{e}_{h}, \mu, \epsilon]$ consist of an incident e(lectron) or h(ole) like quasi-particle in channel μ with energy ϵ superposed with the reflected electron and hole states. The occupation numbers are given by the Fermi-Dirac distribution $f_{e,h} = f(\epsilon \pm eV)$ (the voltage is measured with respect to the chemical potential of the superconductor).

The noise power (1) is determined by the transitions induced by the current operator I from initial states $|n\rangle = |n_n = 1, n_m = 0\rangle$ to intermediate states $|m\rangle = |n_n = 0, n_m = 1\rangle$ and back, which differ only by their occupation with respect to two single particle states with indices n and m. E.g., the transition between an incident electron $n = [e, \nu, \epsilon]$ and an incident hole state $m = [h, \mu, \epsilon]$ is produced by the matrix element between the reflected electrons and holes of the two scattering states with respect to the current operator, $\langle m|I|n\rangle \propto f_e(1 - f_h)(r_{eh}^{\dagger} r_{ee} - r_{hh}^{\dagger} r_{he})_{\mu\nu}$. Summed over the channels, the transitions contribute to the fluctuations with the weight $\sum_{\mu,\nu} |\langle m|I|n\rangle|^2 \propto f_e(1 - f_h)\,\mathrm{Tr}\{(r_{ee}^{\dagger} r_{eh} - r_{he}^{\dagger} r_{hh})(r_{eh}^{\dagger} r_{ee} - r_{hh}^{\dagger} r_{he})\} = f_e(1 - f_h)\,\mathrm{Tr}\{r_{he}^{\dagger} r_{he}(1 - r_{he}^{\dagger} r_{he})\}$. Following the quantum mechanical formalism outlined, we obtain the low-frequency limit of the power spectrum[10] valid for $T \ll eV < \Delta$,

$$P = \frac{4e^2}{h} \int_0^{\Delta} d\epsilon \left\{ [f_e(1 - f_h) + f_h(1 - f_e)]\,\mathrm{Tr}\Big[r_{he}^{\dagger} r_{he} \Big(1 - r_{he}^{\dagger} r_{he}\Big) \Big] + [f_e(1 - f_e) + f_h(1 - f_h)]\,\mathrm{Tr}\Big[\Big(r_{he}^{\dagger} r_{he}\Big)^2 \Big] \right\}. \quad (4)$$

The first term describes the transitions between states of opposite current sign, while the second represents the transitions between states of equal current sign. At zero temperature, the second term is suppressed by the Pauli principle and the first term produces the shot noise[2,11]. The thermal fluctuations describing the Johnson-Nyquist noise[12] are due to both terms. Eq. (4) is manifestly invariant under sign reversal of voltage[13].

Interplay between normal scattering and Andreev reflection. We express the electron-hole reflection matrix $r_{he}(\epsilon)$ in Eq. (4) in terms of the normal reflection- and transmission matrices r_{ii} and t_{ij} of the scattering (X) region and the amplitude of Andreev reflection Γ at the XS interface, $r_{he}(\epsilon) = t_{12}^{*}(-\epsilon)\left[1 - \Gamma^2(\epsilon)\, r_{22}(\epsilon)\, r_{22}^{*}(-\epsilon)\right]^{-1} \Gamma(\epsilon)\, t_{21}(-\epsilon)$ (scattering matrices for X, see Fig. 1: $r_{ii}(\epsilon)$, $t_{ij}(\epsilon)$ for electrons, $r_{ij}^{*}(-\epsilon)$, $t_{ij}^{*}(-\epsilon)$ for holes, $i, j = 1(2)$ left (right), $\Gamma(\epsilon) = e^{i\vartheta(\epsilon)}$, $\vartheta(\epsilon) = \arccos(\epsilon/\Delta)$). Inserting $r_{he}(\epsilon)$ in Eq. 4 provides us with a general multichannel expression for the shot noise in a disordered NXS junction, explicit in the normal scattering matrix and the Andreev reflection amplitude.

Next we restrict ourselves to the situation of a junction with uniform transverse cross-section, which permits the separation of channels and will be used in the single and double barrier systems below. We recall[13] that the differential conductances of the channels $\nu = 1 \ldots N$ are given by the matrix product $r_{he}^{\dagger} r_{he}$ in Eq. (4),

$$\frac{h}{4e^2} G_{\nu}(\epsilon) = \Big(r_{he}^{\dagger} r_{he}\Big)_{\nu\nu} = \frac{T_{\nu}(\epsilon)\, T_{\nu}(-\epsilon)}{T_{\nu}(\epsilon)\, T_{\nu}(-\epsilon) + R_{\nu}(\epsilon) + R_{\nu}(-\epsilon) - 2\mathrm{Re}\Big[\Gamma(\epsilon)^2\, r_{\nu}(\epsilon)\, r_{\nu}^{*}(-\epsilon)\Big]}. \quad (5)$$

$r_{\nu}(\epsilon)$ is the reflection amplitude of channel ν in the matrix $r_{22}(\epsilon)$ describing the reflection from the *right*-hand side of the X region, $R_{\nu}(\epsilon) = |r_{\nu}(\epsilon)|^2$, and $T_{\nu}(\epsilon) = 1 - R_{\nu}(\epsilon)$. The denominator of Eq. (5) contains the interference term describing the iterative scattering processes between the X region and the XS interface. At zero temperature, the shot noise (4) exhibits the noise power $P = \frac{1}{e}\int_0^{e|V|} d\epsilon \sum_{\nu} S_{\nu}(\epsilon)$ with the differential (low-frequency) shot noise of channel ν,

$$\frac{h}{2e^3} S_{\nu}(\epsilon) = 4\Big(r_{he}^{\dagger} r_{he}\Big(1 - r_{he}^{\dagger} r_{he}\Big)\Big)_{\nu\nu} = \frac{4T_{\nu}(\epsilon)\, T_{\nu}(-\epsilon)\Big(R_{\nu}(\epsilon) + R_{\nu}(-\epsilon) - 2\mathrm{Re}\Big[\Gamma(\epsilon)^2\, r_{\nu}(\epsilon)\, r_{\nu}^{*}(-\epsilon)\Big]\Big)}{\Big(T_{\nu}(\epsilon)\, T_{\nu}(-\epsilon) + R_{\nu}(\epsilon) + R_{\nu}(-\epsilon) - 2\mathrm{Re}\Big[\Gamma(\epsilon)^2\, r_{\nu}(\epsilon)\, r_{\nu}^{*}(-\epsilon)\Big]\Big)^2}. \quad (6)$$

The two energy dependencies of the reflection probabilities $R_{\nu}(\epsilon)$ and (the phases of) the reflection amplitudes $r_{\nu}(\epsilon)$ translate into the voltage dependence of the shot noise. The energy dependence of the Andreev amplitude can often be neglected. In the limit $\epsilon \to 0$ ($\Gamma \to -i$) the phase dependencies drop out of Eq. (6) and we recover the linear response result[14] $\left(h/2e^3\right) S_{\nu}(0) = 16T(0)^2[1 - T(0)]/[2 - T(0)]^4$.

NINS junction. In order to decribe the weak coupling of a normal lead to an NS proximity sandwich, we consider a normal-metal – insulator – normal-metal – superconducting (NINS) junction with a potential barrier of low transmission ($T \ll 1$) placed at a distance d away from the perfect NS interface. The NINS junction serves as a model system for a tunneling experiment from a metallic tip to a thin film NS layer structure, which has permitted the observation of the Rowell-McMillan oscillations[15]. In this elementary model, the reflection amplitudes $r_\nu(\epsilon) = \sqrt{R} e^{i\varphi_\nu(\epsilon)}$ have a roughly constant modulus R and an energy dependent phase $\varphi_\nu(\epsilon) \approx 2(k_\nu + \epsilon/v_\nu)d + \varphi_0$, accumulated during the propagation between the potential barrier and the NS interface (k_ν, v_ν denote the Fermi wave number and velocity of channel ν). Consequently the shot noise (6) for the channel ν,

$$\frac{h}{2e^3} S_\nu(\epsilon) = \frac{4T^2 2R\left[1 - \cos\alpha_\nu(\epsilon)\right]}{\left(T^2 + 2R\left[1 - \cos\alpha_\nu(\epsilon)\right]\right)^2}, \tag{7}$$

depends only on the phase difference $\alpha_\nu(\epsilon) = \varphi_\nu(\epsilon) - \varphi_\nu(-\epsilon) - 2\vartheta(\epsilon)$ of electron and hole propagation through the X (=IN) region. The resonance structure of S_ν is intimately connected to the voltage (energy $\epsilon = eV$) dependence of the differential conductance (5),

$$\frac{h}{4e^2} G_\nu(\epsilon) = \frac{T^2}{T^2 + 2R\left[1 - \cos\alpha_\nu(\epsilon)\right]}. \tag{8}$$

Figures 2(a) and 2(b) show their generic dependence on α_ν. The minima of the denominator [$\cos\alpha_\nu = 1 \Rightarrow \epsilon_{\nu,n} = v_\nu/2d(n\pi + \arccos\epsilon_{\nu,n}/\Delta)$] correspond to the resonances of the Andreev quasi-bound states. These conductance resonances are repelled from zero voltage, since the phase of the Andreev reflection $\vartheta(\epsilon \to 0) = \pi/2$ has to be compensated by the phase difference of electron and hole propagation $\varphi_\nu(\epsilon) - \varphi_\nu(-\epsilon)$. The shot noise (7) vanishes at these resonances ($S_\nu(\epsilon_{\nu,n}) = 0$). The noise maxima are found from $\cos\alpha_\nu = \left(2R - T^2\right)/2R$ at energies doubly peaked close to the resonances. The peak separation $\delta\epsilon \sim Tv_F/d$ coincides with the width of the resonances.

Interestingly, this non-trivial structure survives in the multichannel NINS junction, whose results are shown in Figs. 2(d) and 2(e). The stability of the resonance structure is due to its pinning to the Fermi energy. In contrast, the resonance structure of a potential well in a normal conductor is washed out in the multichannel limit. As Figures 2(b,e) show, the narrow double peak structure in the noise is smeared out in the multichannel limit, and the noise S takes a maximum rather than a minimum at the resonance, retracing the shape of the conductance.

At large voltages ($eV \gg v_F/d$), the shot noise approaches a constant as a consequence of the dephasing between the channels. The channel average may be evaluated by averaging over the phase α_ν in Eqs. (7) and (8) and we obtain the result (α_ν $(1/N\sum_n \to 1/2\pi\int_0^{2\pi} d\alpha)$,

$$\bar{S} = \frac{1}{2\pi}\int_0^{2\pi} d\alpha\, S_\nu(\alpha) = \frac{2e^3}{h}T, \qquad \bar{G} = \frac{2e^2}{h}T. \tag{9}$$

It follows that both the shot noise and the conductance approach the normal state values at voltages $v_F/d \ll eV \ll \Delta$. This limiting behavior demonstrates that the NIN junction is effectively decoupled from the NS interface in the large voltage limit and dominates both noise and conductance due to its low transparency.

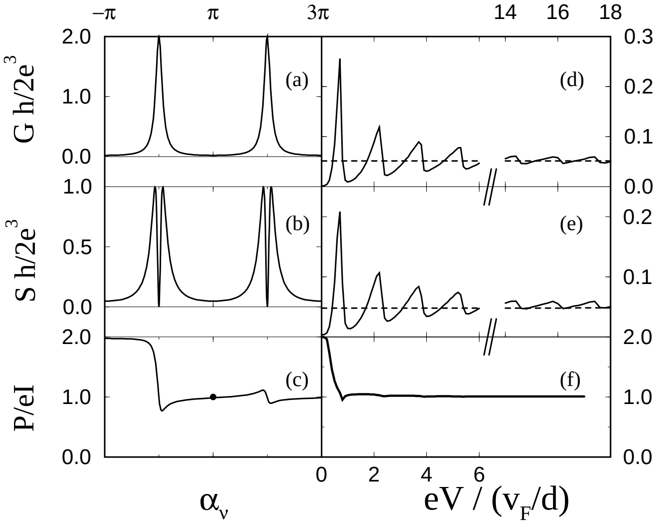

FIG. 2. Zero temperature conductance (a,d), differential shot noise (b,e), and finite voltage noise power to current ratio (c,f) for a NINS junction with a barrier of strength $\int dx\, V(x) = 3\hbar v_F$, average transmission $T = 0.05$, $\epsilon_F = 500\Delta$, $d = 20\, v_F/\Delta$ ($v_F/d \ll \Delta \ll \epsilon_F$). (a,b,c) follow from Eqs. (7) and (8) for one channel. (d,e,f) from Eqs. (5) and (6) are averaged over 8×10^4 channels. Note the pronounced resonance structure in both conductance (d) and noise (e), which approaches the values for the corresponding NIN junction at large voltages (dashed lines). The noise to current ratio (c,f) decays to the classical Schottky value $P/eI = 1$ above the Andreev minigap.

Let us concentrate on the overall ratio of noise power to current P/eI [$P = \int_0^{e|V|} d\epsilon\, S(\epsilon)$, $I = \int_0^{eV} d\epsilon\, G(\epsilon)$]. This ratio has already been used successfully in determining the unit of the charge carriers in the Fractional Quantum Hall Effect[16]. While at small voltages ($P/eI = 2$) the noise carries the signature of the Cooper pairs created by the Andreev reflection, at large voltages ($v_F/d \ll eV \ll \Delta$) it decays to the normal state value ($P/eI = 1$). Interestingly, this decay is immediate at the first Andreev resonance, as is seen from Figs. 2(c) and (f). In fact, in a single channel, the energy integration is equivalent to the integration over the phase α_ν, which at the midpoint between two resonances α_ν has covered the period 2π, thus producing $P/eI = 1$ at $\alpha_\nu = \pi$, see Fig. 2(c). In the transport through a normal lead weakly coupled to a NS sandwich, we thus find two characteristic regimes: At voltages below $eV < v_F/d$ the one-particle excitations in the NS structure are effectively gapped and we may only couple to the superconducting condensate which introduces the charge $2e$ in the noise power. At voltages above the first Andreev resonance, we may couple directly to a one-particle density of states in the normal layer and we loose the signature of the superconductor at once.

Double barrier junction. In the study of normal versus superconducting junctions, it is of interest to investigate the impact the quantum coherence has on the macroscopic limit of transport (limit of an infinite number of channels) and, in particular, to compare the behavior of a specific scattering region connected to either a normal or a superconducting reservoir. We consider an insulator – normal-metal – insulator (X=INI) interferometer which we connect to normal leads in a NININ junction and to a superconducting lead in a NINIS junction. Besides the intrinsic interest in the double barrier system as a paradigm, now to be combined with a superconductor, it may also serve as a qualitative model for a disordered conductor, due to its strong similarity in the transmission distribution[17].

The resonance structure of the INI interferometer results in a bimodal distribution of its (overall) transmission probabilities T. For symmetric barriers it takes the form (infinite channel limit, $T_1 = T_2 \ll 1$)[14],

$$\rho\left(T\right) = \frac{1}{\pi}\frac{T_1}{2}\frac{1}{\sqrt{T^3\left(1-T\right)}}, \qquad T \in \left[\frac{T_1^2}{\pi^2}, 1\right], \tag{10}$$

which has its analog in a disordered conductor[17]. We recall that, in a NININ junction, the rich structure of this distribution has no impact on the macroscopic transport properties. The (linear) conductance and shot noise may be evaluated from the bimodal distribution (10), $\left(h/2e^2\right)G = \int dT\,\rho\left(T\right)T = T_1/2$, $\left(h/2e^3\right)S = \int dT\,\rho\left(T\right)T\left(1-T\right) = T_1/4$, and show no characteristics of coherent transport[18]. The conductance follows from the series resistance of the two barriers, and an incoherent model of a double barrier junction gives the same suppressed noise $S/eG = 1/2$ as a consequence of charge conservation[19]. When considering the INI interferometer in a NINIS junction instead, we find a non-trivial answer, both at small and large voltages. The *linear* response follows from Eqs. (5), (6), and (10),

$$\begin{aligned}
\frac{h}{2e^2}G\left(0\right) &= \int dT\,\rho\left(T\right)\frac{2T^2}{\left(2-T\right)^2} = \frac{T_1}{2}\frac{1}{\sqrt{2}}, \\
\frac{h}{2e^3}S\left(0\right) &= \int dT\,\rho\left(T\right)\frac{16T^2\left(1-T\right)}{\left(2-T\right)^4} = \frac{T_1}{2}\frac{3}{4\sqrt{2}}.
\end{aligned} \tag{11}$$

The ratio of shot noise to conductance is[14] $S\left(0\right)/eG\left(0\right) = 3/4$. A comparison of the shot noise to conductance ratios in a single barrier junction (X=I or X=IN) and a junction with disorder (X=D) is instructive, see Table 1. In the single barrier junction the distribution of transmissions is peaked at $T \ll 1$. The noise is due to the Schottky type fluctuations in nearly closed channels, and consequently the noise ratios $S_N/eG_N = 1$ in the NIN and $S_S/eG_S = 2$ in the NIS junction differ only by the charge quanta involved. In a junction with disorder, the noise-to-conductance ratio is also doubled for the NDS case, see Table 1. However, since in the bimodal distribution of the transmissions the noise is produced by the channels with intermediate transmission $0 < T < 1$ and the current by the open channels with $T \to 1$, the doubling is a non-generic and thus yet unexplained feature. This is demonstrated by the noise-to-conductance ratio of 3/4 in the NINIS as compared to 1/2 in the NININ junction.

At *finite* voltage, the shot noise is described by Eq. (6) with the reflection amplitudes $r_\nu\left(\pm\epsilon\right) = r_2 + t_2^2 r_1 e^{2ik_\nu\left(\pm\epsilon\right)d}/\left(1 - r_1 r_2 e^{2ik_\nu\left(\pm\epsilon\right)d}\right)$ of the double barrier interferometer. We have evaluated this expression for a symmetric double barrier junction ($T_1 = T_2 = 0.05$) and display the results in Fig. 1. At voltages of the order of the Andreev levels $eV \sim v_F/d$, we find a resonance structure independent of the number of channels. We observe again that the differential noise follows the resonance peaks of the conductance. At large voltages ($eV \gg v_F/d$), the resonances disappear as the electrons and holes dephase, and we expect the approach to a regime where the conductance and shot noise become indistinguishable from the incoherent addition of the NIN and NIS junctions.

In conclusion, we have expressed the differential shot noise in a disordered NXS junction in Eq. (6) in terms of the normal and Andreev scattering amplitudes. We have described the resonance structure in the shot noise found at finite voltage in coherent transport. The robustness of the resonance structure in the multichannel limit is owed to its pinning to the Fermi energy. We have pointed out the possibility of a non-trivial normal versus superconducting noise ratio in the NINIS junction as as consequence of the bimodal distribution. Finally, we have found a rapid decay of double shot noise in a NINS junction above the Andreev minigap.

We acknowledge fruitful discussions with D. Agterberg, Ya. M. Blanter, M. Dodgson, and V. B. Geshkenbein. This work has been supported by the Swiss National Science Foundation. G. B. L. acknowledges partial support by RFFRN 96-02-19568.

TABLE I. Shot noise to conductance ratio S/eG of a NXN compared to a NXS junction; single barrier X = I, double barrier X = INI, disorder X = D. The results are valid for small transmissions $T \ll 1$, and many channels $(N \to \infty)^{3,14,18,19}$.

	single barrier $T \ll 1$	double barrier $T_1 = T_2 \ll 1$	disorder
S_N/eG_N	1	1/2	1/3
S_S/eG_S	2	3/4	2/3

APPENDIX:

We diagonalize the BCS-Hamiltonian for superconductivity by a Bogoliubov transformation, considering a spatially inhomogeneous system. The transformation is carried out by determining the quasiparticle wavefunctions that fulfill the Bogoliubov-de-Gennes (BdG) equations. We show that the symmetry in the solutions of the (BdG) equations with respect to reversing the energies $\epsilon_\alpha \to -\epsilon_\alpha$ is a consequence of the spin degeneracy. Making use of the spin-reversal symmetry, we express the Hamiltonian, the density, and the current operators in terms of the quasiparticle operators γ_α, and arrive at the current expression used in Eq. (3).

The mean-field, spin singlet BCS Hamiltonian for superconductivity can be expressed in the form ($h_0 = \left(-i\nabla + e\mathbf{A}\right)^2/2m$)

$$\mathcal{H} = \int d^3x : \hat{\boldsymbol{\Psi}}^\dagger(\mathbf{x}) \begin{pmatrix} h_0 - \mu & \Delta \\ \Delta^* & -h_0^* + \mu \end{pmatrix} \hat{\boldsymbol{\Psi}}(\mathbf{x}) : \tag{A1}$$

using the Nambu spin-up annihilation operator

$$\hat{\boldsymbol{\Psi}}(\mathbf{x}) = \begin{pmatrix} \hat{\Psi}_\uparrow(\mathbf{x}) \\ \hat{\Psi}_\downarrow^\dagger(\mathbf{x}) \end{pmatrix}. \tag{A2}$$

The pair potential is given by $\Delta(\mathbf{x}) = \lambda\langle\hat{\Psi}_\downarrow(\mathbf{x})\,\hat{\Psi}_\uparrow(\mathbf{x})\rangle$ (coupling constant λ), the colon (:) denoting normal ordering with respect to $\hat{\Psi}_\uparrow$ and $\hat{\Psi}_\downarrow$. The Hamiltonian (A1) can be diagonalized by a basis transformation,

$$\hat{\boldsymbol{\Psi}}(\mathbf{x}) = \sum_\alpha \boldsymbol{\Phi}_\alpha(\mathbf{x})\,\gamma_\alpha, \tag{A3}$$

$$\gamma_\alpha = \int d^3x\, \boldsymbol{\Phi}_\alpha^\dagger(\mathbf{x})\,\hat{\boldsymbol{\Psi}}(\mathbf{x}), \tag{A4}$$

with the eigenfunctions $\boldsymbol{\Phi}_\alpha(\mathbf{x})$ of the BdG equations (which follow from the insertion of the Hamiltonian (A1) into $[\mathcal{H}, \gamma_\alpha] = -\epsilon_\alpha\gamma_\alpha$),

$$\begin{pmatrix} h_0 - \mu & \Delta \\ \Delta^* & -h_0^* + \mu \end{pmatrix} \boldsymbol{\Phi}_\alpha(\mathbf{x}) = \epsilon_\alpha \boldsymbol{\Phi}_\alpha(\mathbf{x}), \tag{A5}$$

$$\boldsymbol{\Phi}_\alpha(\mathbf{x}) = \begin{pmatrix} u_\alpha \\ v_\alpha \end{pmatrix}.$$

Note that γ_α are annihilation operators of spin-up states and thus the excitations are all described in terms of spin-up quasiparticles. In order to preserve the (fermionic) commutation relations we need a complete orthonormal set of wavefunctions of the hermitian operator in (A5),

$$\sum_\alpha \boldsymbol{\Phi}_\alpha(\mathbf{x})\,\boldsymbol{\Phi}_\alpha^\dagger(\mathbf{x}') = \mathbf{1}\delta(\mathbf{x} - \mathbf{x}'), \tag{A6}$$

$$\int d^3x\, \boldsymbol{\Phi}_\alpha^\dagger(\mathbf{x})\,\boldsymbol{\Phi}_{\alpha'}(\mathbf{x}) = \delta_{\alpha,\alpha'} \tag{A7}$$

(involving both positive and negative energy eigenstates)[8].

Consider the spin-reversal transformation $\mathcal{S}$,

$$\mathcal{S}\,\hat{\boldsymbol{\Psi}}\,\mathcal{S}^{-1} = \begin{pmatrix} 0 & 1 \\ -1 & 0 \end{pmatrix} \left(\hat{\boldsymbol{\Psi}}^\dagger\right)^\top, \tag{A8}$$

$\mathcal{S}$ linear ($\mathcal{S}\hat{\psi}_\uparrow\mathcal{S}^{-1} = \hat{\psi}_\downarrow$, $\mathcal{S}\hat{\psi}_\downarrow\mathcal{S}^{-1} = -\hat{\psi}_\uparrow$). Noting that the order parameter $\Delta(\mathbf{x})$ is invariant under the transformation (A8), it is easily seen that the Hamiltonian (A1) is spin-reversal symmetric, $[\mathcal{H}, \mathcal{S}] = 0$ (this symmetry extends also to finite magnetic field, if the Zeeman splitting is neglected). By means of spin-reversal we may attribute to each quasi-particle operator γ_α a linearly independent operator $\gamma_{\bar{\alpha}}$ through

$$\gamma_{\bar{\alpha}}^\dagger = \mathcal{S}\gamma_\alpha\mathcal{S}^{-1} = \int d^3x\, \hat{\boldsymbol{\Psi}}^\dagger(\mathbf{x}) \begin{pmatrix} 0 & -1 \\ 1 & 0 \end{pmatrix} \boldsymbol{\Phi}_\alpha^*(\mathbf{x}). \tag{A9}$$

$\gamma_{\bar{\alpha}}$ describes an excitation with opposite energy $\epsilon_{\bar{\alpha}} = -\epsilon_\alpha$ (according to $[\mathcal{H}, \gamma_{\bar{\alpha}}] = \epsilon_\alpha\gamma_{\bar{\alpha}}$). From Eqs. (A9) and (A4) we infer the effect of spin-reversal on the electron-hole wavefunction,

$$\boldsymbol{\Phi}_{\bar{\alpha}}(\mathbf{x}) = \begin{pmatrix} 0 & -1 \\ 1 & 0 \end{pmatrix} \boldsymbol{\Phi}_\alpha^*(\mathbf{x}) = \begin{pmatrix} -v_\alpha^* \\ u_\alpha^* \end{pmatrix}. \tag{A10}$$

We arrive at a complete set of quasi-particle excitations in spin-up space, which are grouped into pairs $\gamma_\alpha, \gamma_{\bar{\alpha}}$ with energies $\pm\epsilon_\alpha$, as a direct consequence of spin degeneracy. Note that within the Nambu picture, all quasiparticles carry spin up [spin ↑ e and spin ↑ h (instead of spin ↓ e)], explaining the opposite energy of the related wavefunction (A10). The Hamiltonian (A1) takes the form,

$$\mathcal{H} = \sum_{\epsilon_\alpha > 0} \epsilon_\alpha \left(\gamma_\alpha^\dagger\gamma_\alpha + \gamma_{\bar{\alpha}}\gamma_{\bar{\alpha}}^\dagger - 2\int d^3x\, |v_\alpha|^2\right). \tag{A11}$$

The ground state is realized by filling all the negative energy quasi-particle states.

The spin-reversal symmetry allows us to express all equations using only half of the eigenstates, i.e., one representative $\boldsymbol{\Phi}_n$ from each pair of states $\{\boldsymbol{\Phi}_\alpha, \boldsymbol{\Phi}_{\bar{\alpha}}\}$. In the following we choose the positive energy eigenstates, expressing the negative energy eigenstates through (A10). We keep the positive energy states for the spin-up quasiparticles ($\gamma_n = \gamma_{n\uparrow}$), and reinterpret the related quasiparticle states of opposite (negative) energy as spin-down excitations ($\gamma_{\bar{n}} = \gamma_{\bar{n}\downarrow}^\dagger$). The Bogoliubov transformation (A3) then takes the well-known form

$$\hat{\boldsymbol{\Psi}}(\mathbf{x}) = \sum_n \begin{pmatrix} u_n \\ v_n \end{pmatrix} \gamma_{n\uparrow} + \begin{pmatrix} -v_n^* \\ u_n^* \end{pmatrix} \gamma_{\bar{n}\downarrow}^\dagger, \tag{A12}$$

and the Hamilton operator is expressed by $\mathcal{H} = \sum_{\epsilon_n > 0} \epsilon_n (\gamma_{n\uparrow}^\dagger\gamma_{n\uparrow} + \gamma_{\bar{n}\downarrow}^\dagger\gamma_{\bar{n}\downarrow} - 2\int d^3x\, |v_n|^2)$, displaying the spin degeneracy in the usual fashion. In the same way, we give the density and current operators in both respresentations, using all (indexed by α) or only the positive energy eigenstates (indexed by n), respectively ($u \overleftrightarrow{\nabla} v = u\nabla v - (\nabla u)v$),

$$
\begin{aligned}
\rho\left(\mathbf{x}\right) &= -e :\hat{\mathbf{\Psi}}^{\dagger}\left(\mathbf{x}\right)\begin{pmatrix} 1 & 0 \\ 0 & -1 \end{pmatrix}\hat{\mathbf{\Psi}}\left(\mathbf{x}\right) := -e\sum_{\alpha,\alpha'}\left(u^{*}_{\alpha}(\mathbf{x})u_{\alpha'}(\mathbf{x})\gamma^{\dagger}_{\alpha}\gamma_{\alpha'} + v^{*}_{\alpha}(\mathbf{x})v_{\alpha'}(\mathbf{x})\gamma_{\alpha'}\gamma^{\dagger}_{\alpha}\right) \qquad (13)\\
&= -e\sum_{\epsilon_m,\epsilon_n>0}\left[u^{*}_{m}(\mathbf{x})u_{n}(\mathbf{x}) - v^{*}_{m}(\mathbf{x})v_{n}(\mathbf{x})\right]\left(\gamma^{\dagger}_{m\uparrow}\gamma_{n\uparrow} + \gamma^{\dagger}_{\bar{m}\downarrow}\gamma_{\bar{n}\downarrow}\right) - 2e\sum_{\epsilon_n>0}|v_n(\mathbf{x})|^2\\
&\quad -e\sum_{\epsilon_m,\epsilon_n>0}\left\{\left[u_m(\mathbf{x})v_n(\mathbf{x}) + v_m(\mathbf{x})u_n(\mathbf{x})\right]\gamma_{m\uparrow}\gamma_{\bar{n}\downarrow} + \text{ h.c. }\right\}, \qquad (14)
\end{aligned}
$$

$$
\begin{aligned}
\mathbf{j}\left(\mathbf{x}\right) &= -\frac{e}{2mi} :\hat{\mathbf{\Psi}}^{\dagger}\left(\mathbf{x}\right)\overleftrightarrow{\nabla}\hat{\mathbf{\Psi}}\left(\mathbf{x}\right) := -\frac{e}{2mi}\sum_{\alpha,\alpha'} u^{*}_{\alpha}(\mathbf{x})\overleftrightarrow{\nabla}u_{\alpha'}(\mathbf{x})\gamma^{\dagger}_{\alpha}\gamma_{\alpha'} - v^{*}_{\alpha}(\mathbf{x})\overleftrightarrow{\nabla}v_{\alpha'}(\mathbf{x})\gamma_{\alpha'}\gamma^{\dagger}_{\alpha} \qquad (15)\\
&= -\frac{e}{2mi}\left\{\sum_{\epsilon_m,\epsilon_n>0}\left(u^{*}_{m}(\mathbf{x})\overleftrightarrow{\nabla}u_{n}(\mathbf{x}) + v^{*}_{m}(\mathbf{x})\overleftrightarrow{\nabla}v_{n}(\mathbf{x})\right)\left(\gamma^{\dagger}_{m\uparrow}\gamma_{n\uparrow} + \gamma^{\dagger}_{\bar{m}\downarrow}\gamma_{\bar{n}\downarrow}\right) - 2\sum_{\epsilon_n>0}v^{*}_{n}(\mathbf{x})\overleftrightarrow{\nabla}v_{n}(\mathbf{x})\right\}\\
&\quad -\frac{e}{2mi}\sum_{\epsilon_m,\epsilon_n>0}\left\{\left(-u_m(\mathbf{x})\overleftrightarrow{\nabla}v_n(\mathbf{x}) + v_m(\mathbf{x})\overleftrightarrow{\nabla}u_n(\mathbf{x})\right)\gamma_{m\uparrow}\gamma_{\bar{n}\downarrow} - \text{ h.c. }\right\}. \qquad (16)
\end{aligned}
$$

The current operator is easily generalized to finite magnetic field. We note that current and density operators obey the continuity equation

$$
\frac{\partial\rho(\mathbf{x})}{\partial t} + \nabla\cdot\mathbf{j}(\mathbf{x}) = 2ie\hat{\mathbf{\Psi}}^{\dagger}\left(\mathbf{x}\right)\begin{pmatrix} 0 & \Delta(\mathbf{x}) \\ -\Delta^{*}(\mathbf{x}) & 0 \end{pmatrix}\hat{\mathbf{\Psi}}\left(\mathbf{x}\right), \qquad (17)
$$

where the right hand side vanishes when taking the (self-consistent) expectation value. The effective current expression used as a starting point in Eq. (3) is obtained from (16), accounting for the spin degeneracy by a factor 2 and dropping the particle non-conserving last term, which is eliminated by the frequency integration in (1).

---

[1] W. Schottky, Ann. Phys. **57**, 541 (1918).

[2] G. B. Lesovik, JETP Lett. **49**, 592 (1989); M. Büttiker, Phys. Rev. B **46**, 12485 (1992)..

[3] V. A. Khlus, Zh. Eksp. Teor. Fiz. **93**, 2179 (1987) [Sov. Phys. JETP **66**, 1243 (1987)].

[4] B. A. Muzykantskii and D. E. Khmelnitskii, Phys. Rev. B **50**, 3982 (1994).

[5] M. J. M. de Jong and C. W. J. Beenakker, Phys. Rev. B **49**, 16 070 (1994).

[6] J. P. Hessling *et al.*, Europhys. Lett. **34**, 49 (1996).

[7] D. Averin and H. T. Imam, Phys. Rev. Lett. **76**, 3814 (1996); P. Dieleman, H. G. Bukkems, T. M. Klapwijk, M. Shicke, and K. H. Gundlach, cond-mat/9709030.

[8] V. Niño C. and R. Kümmel, Phys. Rev. B **29**, 3957 (1984).

[9] We use the notation of Ref.[13], with the only change, that the global reflection amplitudes are denoted by lower-case instead of capital letters, e.g., r_{he} instead of R_{he}.

[10] M. P. Anantram and S. Datta, Phys. Rev. B **53**, 16 390 (1996); T. Martin, Phys. Lett. A **220**, 137 (1996).

[11] G. B. Lesovik and L. S. Levitov, Phys. Rev. Lett. **72**, 724 (1994); L. S. Levitov, H. Lee, and G. B. Lesovik, J. Math. Phys. **37**, 4845 (1996).

[12] M. B. Johnson, Phys. Rev. **29**, 367 (1927); H. Nyquist, *ibid.* **32**, 110 (1928).

[13] G. B. Lesovik, A. L. Fauchère, and G. Blatter, Phys. Rev. B **55**, 3146 (1997).

[14] M. J. M. de Jong and C. W. J. Beenakker, in *Mesoscopic Electron Transport*, eds. L. Sohn *et al.*, Kluwer Academic 1997.

[15] J. M. Rowell and W. L. McMillan, Phys. Rev. Lett. **16** 453 (1966).

[16] L. Saminadayar, D. C. Glattli, Y. Jin, and B. Etienne, Phys. Rev. Lett. **79**, 2526 (1997); R. de-Picciotto, M. Reznikov, M. Heiblum, V. Umansky, G. Bunin, and D. Mahalu, cond-mat/9707289.

[17] O. N. Dorokhov, JETP Lett. **36**, 318 (1982); J. A. Melson, C. W. J. Beenakker, Physica B **203**, 219 (1994).

[18] L.Y. Chen and C.S. Ting, Phys. Rev. B **43**, 4534 (1991).

[19] C. W. J. Beenakker and M. Büttiker, Phys. Rev. B **46**, 1889 (1992).